An Evolutionary Approach, B. D. Roitberg and M. B. Isman, Eds. (Routledge, Chapman and Hall, New York, 1992), pp. 89–121.
45. Seminal studies of highly elaborate insect-angiosperm associations include P. R. Ehrlich and P. H. Raven, *Evolution* **18**, 586 (1964); D. H. Janzen, *ibid.* **20**, 249 (1966); V. F. Eastop, *Symp. R. Entomol. Soc. London* **6**, 157 (1972); ______ and M. Berenbaum, *Evolution* **37**, 163 (1983). Recent studies have shown that compared to their nonherbivorous sister groups, many lineages of herbivorous insects have preferentially diversified with angiosperms [C. Mitter, B. Farrell, B. Weigman, *Am. Nat.* **132**, 107 (1988); C. Mitter, B. Farrell, D. J. Futuyma, *Trends Ecol. Evol.* **6**, 290 (1991)] and, conversely, that relatively insect-resistant latex-bearing angiosperm lineages have preferentially diversified compared to their non–latex-bearing sister groups [B. D. Farrell, D. E. Dussourd, C. Mitter, *Am. Nat.* **138**, 881 (1991)].
46. J. J. Sepkoski, Jr., *Paleobiology* **5**, 222 (1979); *Short Courses Paleontol.* **4**, 136 (1991).
47. B. B. Rohdendorf, Ed., *Jurassic Insects of Karatau* (in Russian) (Izdatelstvo "Nauka," Moscow, 1968); A. P. Rasnitsyn, *Trans. Paleontol. Inst.* **174**, 1 (1980); N. S. Kalugina and V. G. Kovalev, *Dipterous Insects from the Jurassic of Siberia* (in Russian) (Izdatelstvo "Nauka," Moscow, 1985); L. V. Arnol'di, V. V. Zherikin, L. M. Nikritkhin, A. G. Ponomarenko, *Mesozoic Coleoptera* (Smithsonian Institution Library and National Science Foundation, Washington, DC, 1991).
48. P. Whalley, *Nature* **327**, 562 (1987); E. A. Jarembowski, *Mesozoic Res.* **2**, 25 (1989); C. C. Labandeira, *Paleontol. Soc. Spec. Publ.* **6**, 174 (1992); E. M. Pike, *ibid.*, p. 234.
49. N. F. Hughes and A. B. McDougall, *Rev. Palaeobot. Palynol.* **50**, 255 (1987).
50. J. A. Doyle and M. J. Donaghue, *Bot. Rev.* **52**, 321 (1986); *Paleobiology* **19**, 141 (1993).
51. S. Lidgard and P. R. Crane, *Nature* **331**, 344 (1988).
52. See also K. J. Niklas, *Brittonia* **30**, 373 (1978); P. R. Crane, *Ann. Mo. Bot. Gard.* **72**, 716 (1985); and O. Pellmyr, *Trends Ecol. Evol.* **7**, 46 (1992).
53. A. C. Rozefelds, *Proc. R. Soc. Queensl.* **99**, 77 (1988); A. J. Boucot, *Evolutionary Paleobiology of Behavior and Coevolution* (Elsevier, Amsterdam, 1990); C. C. Labandeira and B. S. Beall, *Short Courses Paleontol.* **3**, 214 (1990).
54. Low estimates, or minimum ages, are derived from direct evidence of the body-fossil record. High estimates are determined from more indirect lines of evidence: trace fossils, fossil presence of a conspecific developmental (that is, ontogenetic) stage other than the one being analyzed, and inferred presence due to sister-group relationships from cladistic studies.
55. Data on insect family ranges and mouthpart classes are available from C.C.L. We thank D. Chaney and F. Marsh for assistance in drafting the figures and D. H. Erwin, D. J. Futuyma, J. Kukalová-Peck, and A. P. Rasnitsyn for critical commentary. Research received support from the National Aeronautics and Space Administration under grants NAG 2-282 and NAGW-1693 to J.J.S. This is Evolution of Terrestrial Ecosystems Contribution no. 12.

A Cold Suboceanic Mantle Belt at the Earth's Equator

Enrico Bonatti, Monique Seyler, Nadia Sushevskaya

An exceptionally low degree of melting of the upper mantle in the equatorial part of the mid-Atlantic Ridge is indicated by the chemical composition of mantle-derived mid-ocean ridge peridotites and basalts. These data imply that mantle temperatures below the equatorial Atlantic are at least ~150°C cooler than those below the normal mid-Atlantic Ridge, suggesting that isotherms are depressed and the mantle is downwelling in the equatorial Atlantic. An equatorial minimum of the zero-age crustal elevation of the East Pacific Rise suggests a similar situation in the Pacific. If so, an oceanic upper mantle cold equatorial belt separates hotter mantle regimes and perhaps distinct chemical and isotopic domains in the Northern and Southern hemispheres. Gravity data suggest the presence of high density material in the oceanic equatorial upper mantle, which is consistent with its inferred low temperature and undepleted composition. The equatorial distribution of cold, dense upper mantle may be ultimately an effect of the Earth's rotation.

A basic tenet of the theory of plate tectonics states that upper mantle isotherms rise beneath mid-ocean ridges because of the upwelling of hot mantle material, which as a result undergoes partial melting. The melt fraction migrates upward, cools, and forms the oceanic crust. The degree of melting undergone by mantle peridotites upwelling beneath mid-ocean ridges can be estimated either from the chemical composition of the melt fraction (mid-ocean ridge basalts or MORBs) or the solid residue left behind after partial melting (mid-ocean ridge peridotites or MORPs). These estimates are based on experimental work on the melting of peridotites under different pressure and temperature conditions (*1, 2*) and on assumptions as to the initial composition of the upwelling upper mantle material (*1, 3*). Estimates based on the composition of peridotite samples recovered along the mid-Atlantic Ridge (MAR) suggest that the degree of melting of the upper mantle along the MAR ranges from ~8 to ~25% and varies regionally over long (~1000 km) and short (~100 km) scales (*4–6*). Estimates derived independently from the composition of MORBs (*7*) agree in general with those obtained from MORPs.

Recent studies of MORPs and MORBs from the central MAR have suggested that the upper mantle in some areas of the equatorial Atlantic has undergone little or no melting; thus, the mantle appears to be relatively cold in these areas (*6, 8*). We present additional data and discuss possible causes and implications of an equatorial belt of cold upper mantle in the Atlantic and east Pacific.

E. Bonatti is at the Lamont-Doherty Earth Observatory, Columbia University, Palisades, NY 10964 and the Istituto Geologia Marina CNR, Bologna, Italy. M. Seyler is at the Laboratoire de Petrologie, Université Lille, Lille, France. N. Sushevskaya is at the Vernadsky Institute of Geochemistry, Russian Academy of Sciences, Moscow, Russia.

Partial Melting of Atlantic Mantle Peridotites

The mantle-equilibrated minerals found in MORPs include olivine (ol), orthopyroxene (opx), clinopyroxene (cpx), and spinel (sp). The composition of these phases has been determined in many peridotites from the north and equatorial Atlantic (*5, 6, 9, 10*). Peridotites from the equatorial region are of particular interest in this context. Near the equator, the MAR axis is offset by major transform faults, including the Romanche fracture zone (FZ) (~950-km offset) at the equator, the St. Paul FZ just north of the equator, and the Chain FZ just south of it (Fig. 1).

We found that the composition of peridotites sampled from several sites along the Romanche FZ (Fig. 1) is different from that of other MORPs. For instance, their mantle-equilibrated phases have higher concentrations of incompatible elements (elements such as Al that partition with the melt) and lower concentrations of refractory elements (elements such as Mg and Cr that stay with the solid residue during partial melting) than MORPs from the Atlantic and Indian oceans (Fig. 2). Representative samples show a modal content of clinopyroxene higher than that of other MORPs (Fig. 3).

Laboratory experiments and theoretical modeling show that the modal and mineral composition of mantle peridotites changes as a result of partial melting (*1, 2, 11*). Assuming an initial pyrolitic modal composition for parental upper mantle beneath the ridge (*3*), partial melting at 10 kbar causes a rapid decrease in the content of clinopyroxene (and eventually its disappearance when the degree of melting is over about 20%), a slower decrease of orthopyroxene, and an increase of olivine (*1, 2*). Moreover, the initial chemical composition of the primary phases is modified by partial melting, so that the ratio of refractory elements to incompatible elements increases with an increased degree of melting (*1, 2*).

The low ratio of refractory to incompatible elements of the Romanche peridotites relative to MORPs from the Atlantic and Indian oceans implies that the Romanche peridotites have undergone a low degree of melting. We can estimate the degree of melting by assuming a source mantle of "pyrolitic" composition (*3*) and calibrating the mineral chemistry data with the experimental results (*1*, *11*). The estimated degrees of melting are probably higher than the average degree of melting for the mantle column above the depth of the solidus because these estimates are based on peridotites sampled from near the top of the column, which have undergone the largest decompression and, therefore, the highest degree of melting.

Evidence from MORPs. Out of over 150 analyzed peridotites from over 50 sites in the Atlantic, spinel 100Cr/(Cr + Al) values <13 (<5% melting under the usual assumptions) were obtained at four sites in the Romanche FZ but only at two sites outside the Romanche FZ; both sites (one on the St. Paul FZ, the other at the Chain FZ) are close to the equator. Two of the most undepleted samples (AT196AE and AT196M) were recovered from a site in the western part of the Romanche transform valley, about 60 km from the intersection of the MAR and the transform (Fig. 1). The modal (*12*) and bulk chemical compositions of these samples (Table 1) are similar to those estimated for pyrolite (Fig. 3). The spinel 100Cr/(Cr + Al) ratio (~10), the orthopyroxene and clinopyroxene Al_2O_3 contents (~5.8 to 6.0% and 7.5 to 7.8%, respectively), and the Ti/Zr ratio in clinopyroxene (~150 to 170) are all close to the estimated values for pyrolite (Fig. 2) and other undepleted mantle samples, such as the Tinaquillo peridotite (*1*), the Zabargad spinel lherzolites (*13*), fertile xenoliths (*14*), and undepleted xenoliths from San Carlos, Arizona (*15*). The modal compositions of samples AT196AE and AT196M, with 14% and 12% clinopyroxene, respectively (*12*), are also close to those of the fertile peridotites quoted above (Fig. 3). These samples are not depleted peridotites refertilized by a basaltic melt (*16*); their low spinel 100Cr/(Cr + Al) ratios contrast with high ratios in spinel of peridotites that have reacted with a basaltic melt (*6*, *17*, *18*).

The data shown in Table 1 and Figs. 2 and 3 indicate that samples AT196AE and AT196M are similar to what we expect parental oceanic mantle to look like: that is, mantle that has not undergone any significant partial melting in a sub–mid-ocean ridge thermal regime. These samples are not flukes: peridotites recovered from three other sites in the western Romanche are also less depleted than Atlantic and Indian ocean MORPs (Figs. 1 and 2).

Peridotites from the eastern part of the Romanche transform give a more complex picture. Most samples contain traces of plagioclase (plag) and have anomalous mineral composition, such as spinel enriched with Fe and Ti, and clinopyroxene enriched with light rare earth elements (LREE). Spinel in these samples is not only Fe- and Ti-rich but has also a high (>40) 100Cr/(Cr + Al) ratio (Fig. 2).

One possible explanation is that these peridotites have reacted at mantle levels either with a trapped basaltic melt (*6*, *18*, *19*) or with a metasomatic fluid in narrow (1 to 10 cm) mantle shear zones, as has been observed in several peridotite massifs exposed on land (*13*, *20*). The injection of fluids into narrow shear zones in peridotite in the shallow mantle could (i) lower locally the solidus temperature, which may or may not result in localized incipient melting; (ii) induce recrystallization at low pres-

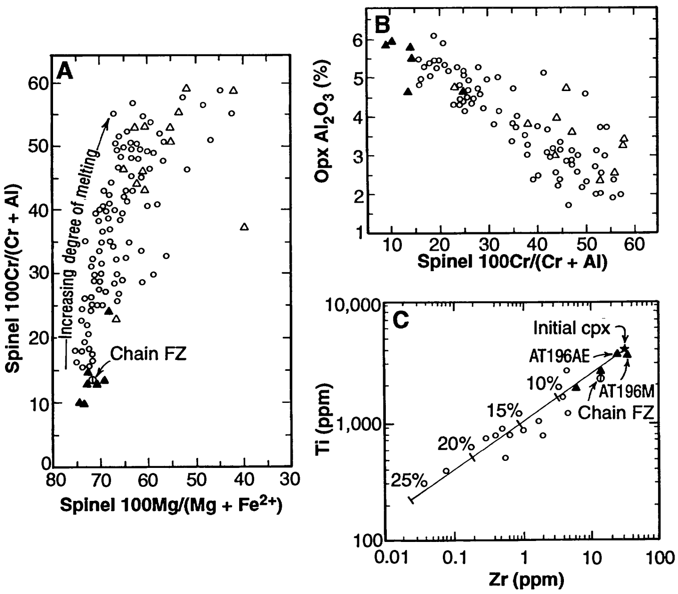

Fig. 2. Mineral chemical composition of North Atlantic MORPs (circles). Data from Romanche FZ marked by solid triangles. (**A**) Spinel 100Cr/(Cr + Al) versus 100Mg/(Mg + Fe^{2+}). The 100Cr/(Cr + Al) ratio increases with increasing extent of melting. However, it also increases in peridotites that have undergone reactions with metasomatic fluids or melts, as discussed in the text. Open triangles indicate Romanche FZ peridotites with evidence of such secondary metasomatic reactions. (**B**) Al_2O_3 in orthopyroxene versus 100Cr/(Cr + Al) in spinel of Romanche and North Atlantic MORPs (*9*). (**C**) Ti/Zr of clinopyroxene of North Atlantic MORPs analyzed by ion probe (*9*). Line, originating at the star, indicates increasing degrees of fractional partial melting from a parental clinopyroxene, according to Johnson *et al.* (*11*).

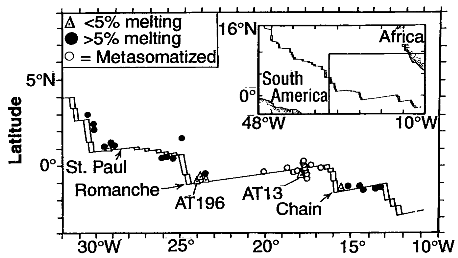

Fig. 1. Schematic ridge-transform geometry in the equatorial Atlantic. Sites where peridotite samples were recovered are indicated. Different types of peridotites are shown with different symbols. Most of the sites at the Romanche FZ yielded either undepleted peridotites or peridotites that have reacted with a metasomatic fluid or melt.

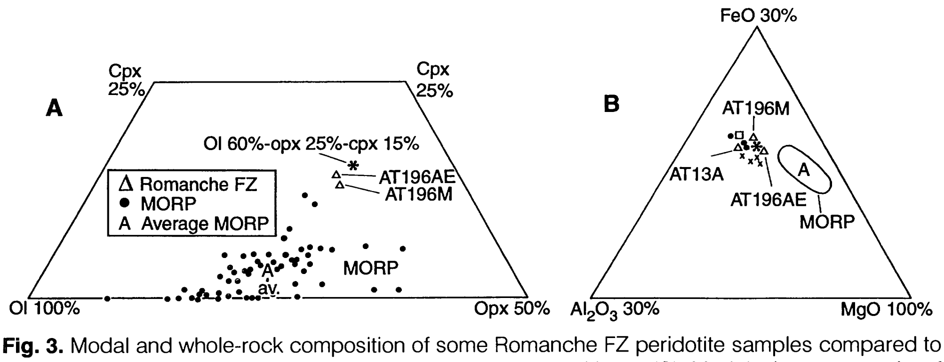

Fig. 3. Modal and whole-rock composition of some Romanche FZ peridotite samples compared to MORPs and to pyrolite (*3*) and other undepleted compositions. (**A**) Modal ol:opx:cpx ratio of samples AT196AE and AT196M compared with Atlantic and Indian Ocean MORPs (*4*, *5*) and to an undepleted composition close to pyrolite (*). (**B**) Whole-rock MgO:Al_2O_3:FeO* ratio (FeO*, total iron expressed as FeO) of samples AT196AE and AT196M (western Romanche FZ) and AT13A (eastern Romanche FZ) compared to pyrolite (*) (*3*), Zabargad spinel lherzolites (×) (*13*), fertile xenoliths (●) (*14*), a San Carlos fertile xenolith (□) (*15*), average abyssal peridotite (A) (*4*), and a MORP field.

sure through reactions such as opx + cpx + Al-spinel → ol + plag + Cr-spinel (*21*); and (iii) introduce Fe, Ti, LREE, and other trace elements into the peridotite. This process of metasomatism could account for the "enriched" chemistry of spinel and clinopyroxene. Reactions between peridotite and trapped melt or peridotite and fluid as well as recrystallization at low pressure all modify the chemistry of the primary mantle minerals: for instance, such reactions tend to lead to an increase of the Cr/Al ratio of spinel (*6, 17, 18*). These changes make it difficult to estimate the degree of depletion and of partial melting undergone by these peridotites by calibration of their mineral chemistry with experimental data.

If the trapped melt explanation is valid, the trapped melt represents either incipient melting of the host peridotite or a migrating melt from deeper in the upper mantle. Regardless of its origin, the presence of a melt fraction in mantle peridotite may indicate that the lithospheric mantle is cold enough to freeze and trap any small amount of melt produced within it or migrating through it (*19*). If instead the plagioclase peridotites represent subsolidus, low-pressure recrystallization, a relatively cold upper mantle regime is also implied. The extent of melting achieved under normal mid-ocean ridge conditions by the time the pressure of plagioclase stability is reached (~8 kbar) is likely to exceed the amount of melting that would allow plagioclase in the residue. It is only in the coldest regions (smallest extent of melting) that plagioclase may remain in the residue (*7*). Thus, the presence of plagioclase peridotites, regardless of their origin, implies that the local upper mantle regime was cold. Plagioclase peridotites have rarely been found among MORPs in the North Atlantic but are abundant in the equatorial Atlantic region (*18*).

That the eastern Romanche peridotites also underwent a low degree of melting is suggested by the chemistry of a few plagioclase-free samples that appear not to have been affected by secondary reactions. One such sample, AT13A (Fig. 1), recovered from the southern wall of the transform valley, shows a low spinel 100Cr/(Cr + Al) ratio (~13) and high Al content in orthopyroxene and clinopyroxene. These features are indicative of a degree of melting as low as that of the western Romanche samples, lower than other Atlantic MORPs (*22*).

Evidence from MORBs. We conclude that the little or no melting documented for the Romanche upper mantle indicates that an upper mantle belt along the equatorial Atlantic is exceptionally cold. Independent support for this conclusion is derived from studies of MAR basalts. Schilling *et al.* (*8*) have suggested that equatorial Atlantic MORBs are produced by a low degree of melting, thus a relatively low temperature of their mantle source. Klein and Langmuir (*7*) have demonstrated that the degree of melting of MORB mantle source can be estimated from the chemical composition of the melt. They showed that the Na and Fe contents of fresh MORBs, normalized at 8% MgO to correct for the effects of fractionation (Na8 and Fe8), are related to the degree and pressure of melting of the mantle source. We have analyzed fresh MORB glasses from the equatorial MAR (*23*).

The Na8 and $Fe^{G}8$ values of these MORBs indicate a minimum in the degree of melting of the source near the equator compared with that from higher latitudes along the MAR (*7, 24–26*) (Fig. 4). The distribution of MORBs with high Na8 and low $Fe^{G}8$ values complements that of MORPs with low spinel 100Cr/(Cr + Al) ratios and provides independent support for a low degree of melting of the equatorial MORB source, and thus for a low temperature of the equatorial Atlantic upper mantle.

Nepheline-normative, LREE-enriched alkali basalts, different in composition from MORBs, have been recovered at several sites in the equatorial Atlantic (*27–29*), although they are exceedingly rare elsewhere in the MAR. They are probably produced by low degrees of melting in the mantle and are consistent with the idea that the equatorial Atlantic upper mantle is relatively cold.

Geophysical evidence. The idea of cold equatorial upper mantle under the Atlantic is supported by geophysical parameters such as zero-age crustal depth below sea level and seismic S-wave velocities. Mid-ocean ridges show an inverse relation between zero-age depth below sea level and degree of melting (*7*). Zero-age depth of the MAR axis reaches a maximum in the equatorial area (Fig. 4). High-resolution seismic S-wave tomography along the MAR (*30*) shows a relatively high velocity (low temperature) zone in the equatorial region (Fig. 4), in agreement with the geochemical results.

On the basis of the calibration of the major element composition of spinel, ortho-

Table 1. Major element whole-rock and mineral analyses of peridotite samples AT196AE and AT196M. Whole-rock analyses by x-ray fluorescence (*10*). Mineral analyses carried out with L-DEO Camebax electron probe (*10*). Cation composition is also given. Abbreviations: LOI, loss on ignition; Mg* = 100 Mg/(Mg + Fe); Cr* = 100 Cr/(Cr + Al).

	AT196AE					AT196M				
	Whole rock (%)	Ol (%)	Opx (%)	Cpx (%)	Sp (%)	Whole rock (%)	Ol (%)	Opx (%)	Cpx (%)	Sp (%)
SiO_2	42.32	41.05	54.20	51.34		43.00	41.04	54.11	50.68	
TiO_2	0.09		0.16	0.53	0.05	0.13		0.14	0.64	0.02
Al_2O_3	2.91	0.03	5.99	7.78	58.53	3.76		5.81	7.55	57.11
Cr_2O_3	0.36		0.53	0.88	9.81	0.37		0.47	0.55	9.80
Fe_2O_3	9.11				0.0	9.05				1.49
FeO		9.86	6.29	2.79	11.87		10.02	6.79	2.93	11.36
MnO	0.13	0.14	0.14	0.06		0.12	0.12	0.12	0.09	
MgO	37.41	47.60	30.59	14.29	18.49	36.99	48.78	32.02	15.35	19.14
CaO	2.28	0.01	1.25	20.42		2.67	0.02	0.81	22.36	
Na_2O	0.37		0.06	1.34		0.25		0.02	0.71	
K_2O	0.02					0.05				
NiO	0.29	0.37	0.06	0.04	0.35	0.26	0.42			0.40
LOI	4.38					3.51				
Total	99.68	99.07	99.27	99.46	99.11	100.16	100.40	100.29	100.86	99.32
Si		1.015	1.888	1.865			1.002	1.868	1.822	
Ti			0.004	0.015	0.008			0.004	0.017	0.003
Al		0.001	0.246	0.333	14.425			0.236	0.320	14.095
Cr			0.015	0.025	1.622			0.013	0.016	1.623
Fe		0.204	0.183	0.085			0.205	0.196	0.088	
Fe_3					0.000					0.234
Fe_2					2.076					1.990
Mn		0.003	0.004	0.002			0.003	0.004	0.003	
Mg		1.754	1.588	0.773	5.763		1.776	1.648	0.823	5.975
Ca		0.000	0.047	0.795			0.001	0.030	0.861	
Na			0.004	0.095				0.001	0.050	
Ni		0.007	0.002	0.001	0.059		0.008			0.067
Total		2.984	3.981	3.989	23.953		2.995	4.000	4.000	23.753
Cr*					10.1					10.3
Mg*		89.1	89.4	89.9	74.5		89.2	83.2	90.0	72.7
Wollastonite			2.56	48.03				1.60	48.60	
Enstatite			87.16	46.74				87.94	46.43	
Ferrosilite			10.28	5.23				10.46	4.97	

pyroxene, and olivine and trace elements in clinopyroxene of MORPs with experimental values (*1, 2, 11*), the degree of melting for the equatorial Atlantic upper mantle is ~5%, compared with ~10 to 15% for MORPs elsewhere in the North Atlantic, except for anomalous hot spots at 35° to 45°N, 15°N, and 2° to 4°N, where it can reach over 20% (*4–6*). Assuming that these differences in degree of melting are caused solely by differences in upper mantle temperatures, following McKenzie (*31*) and Klein and Langmuir (*7*), we estimate that temperatures in the melting region of the equatorial mantle are at least 150°C lower than elsewhere in the MAR (excluding hot spots).

Can this cold equatorial mantle reflect a transform cold edge effect (*32*), the cooling of the MAR as it lies against old, cold, and thick lithosphere of the Romanche long offset transform? If the ridge-transform geometry in the Romanche region is more or less permanent and the average spreading rates are 1.70 cm/year on both sides of the transform (*33*), the lithosphere being impinged by the MAR axis at both MAR-transform intersections is about 50 million years old. The oceanic lithosphere thickens and cools in proportion to the square root of its age (*33, 34*). Accordingly, rapid thickening and cooling occurs only in the first few million years after the formation of the lithosphere at the ridge axis. Thus, the magnitude of the cold edge effect should be not very different among slow slip transforms for which the age offset is >20 million years. However, mantle peridotites from Atlantic transform zones with similar age offsets show a wide range in the degree of melting. Similarly, the relative degree of depletion of North Atlantic peridotites [expressed by spinel 100Cr/(Cr + Al)] does not vary inversely with the length of offset of North Atlantic transforms, as would be expected if the cold edge effect were a major factor in the determination of the degree of depletion of the upper mantle (Fig. 5). Instead, strongly depleted peridotites [100Cr/(Cr + Al) > 40] are exclusively from known hot spot regions (Azores, 15°20′N, and 2° to 3°N), regardless of the length of transform offset. Compositions of MORBs also do not show a systematic transform cold edge effect (*35*). Thus, it is unlikely that the transform cold edge effect is the main cause of the anomalously cold equatorial mantle.

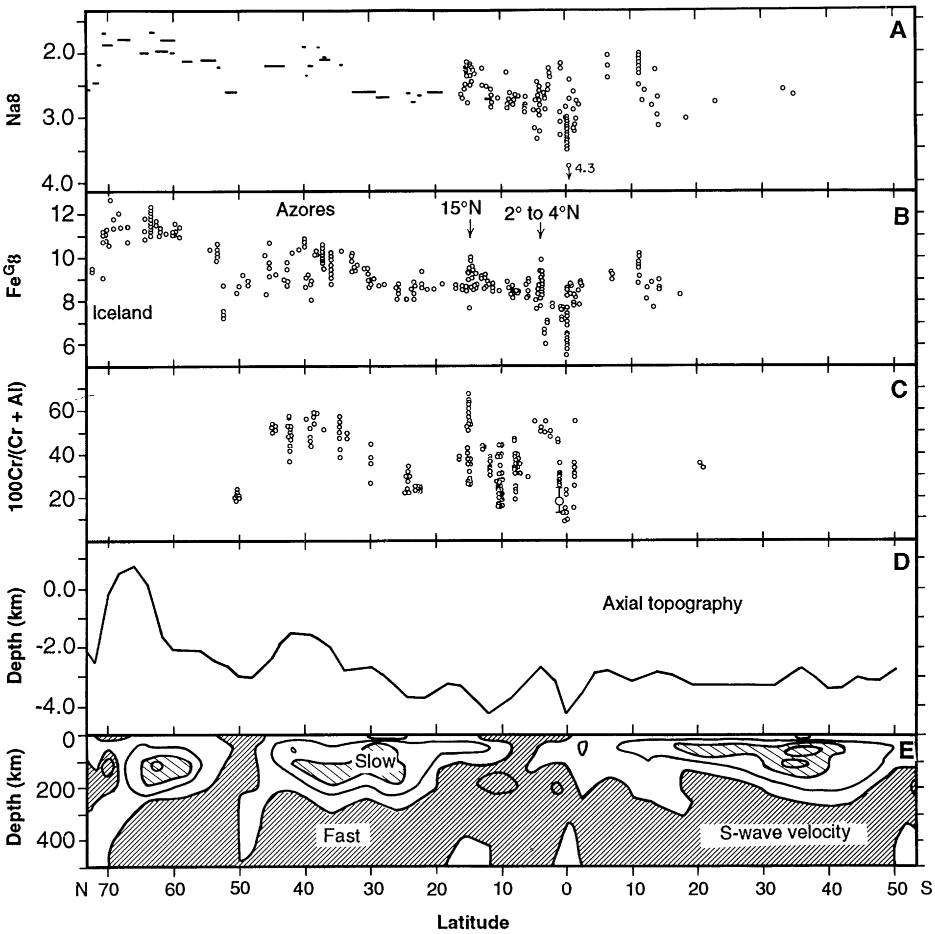

Fig. 4. Variation with latitude of geochemical and geophysical parameters along the MAR. (**A**) Zero-age MORB Na8 and (**B**) Fe^{G}8. Data other than our own from (*7, 24, 26*). Hot spots indicated at Iceland, Azores, 15°N, and 2° to 4°N. (**C**) Spinel 100Cr/(Cr + Al) in peridotites sampled from the MAR (*9*). Samples are from mantle-derived peridotite bodies in transform valley walls, axial valley walls, and a few sites off the ridge axis. Samples showing evidence of metasomatic reactions have not been included. Large circle indicates peridotites from St. Peter Paul Island. (**D**) Zero-age depth relative to sea level along MAR (*30*). (**E**) Variation of S-wave seismic velocity with depth and latitude (*30*).

Equatorial Belt of Downwelling Mantle Isotherms

If the cold equatorial Atlantic upper mantle reflects some property or process with a latitudinal symmetry, the equatorial cold upper mantle should not be restricted to the Atlantic but should be observed also in the other major oceans. Evidence from the other oceans is consistent with the hypothesis, although less compelling than that obtained from the Atlantic.

Contrary to the case of the MAR, petrological data that allow independent estimates of upper mantle temperature variations along the equatorial East Pacific Rise (EPR) are lacking (*36*). However, topographic evidence suggests that there is an equatorial thermal minimum at the EPR and possibly at the mid-Indian Ridge. The topography of the crest of the EPR and of the other mid-ocean ridges depends on latitude (*37*). Ridge-crest elevations in the equatorial zone are several hundred meters deeper than at high latitudes. In the Pacific, the zero-age equatorial minimum can be

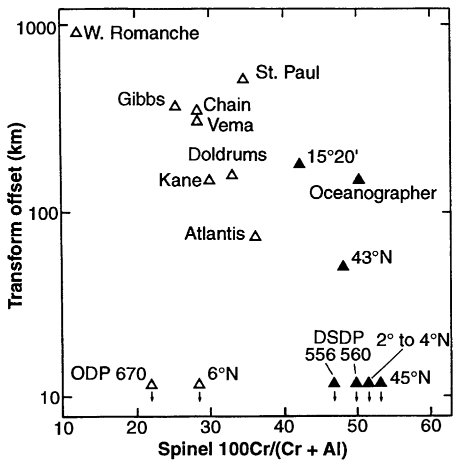

Fig. 5. Average spinel 100Cr/(Cr + Al) ratio of peridotite versus length of transform offsets for the North Atlantic. Points at the bottom with arrows indicate peridotites from the MAR axis or other areas not on a transform or fracture zone, where the length of offset is zero. Samples from regions of known hot spots [35° to 45°N (Azores), 15°N, and 2° to 4°N] are indicated by filled symbols. Peridotites with high values (>40) of spinel 100Cr/(Cr + Al) are exclusively from hot spot areas, regardless of length of offset. ODP, Ocean Drilling Project; DSDP, Deep Sea Drilling Project.

extended back in time (Fig. 6). Menard and Dorman (*37*) were able to expand the age-depth relation attributable to thermal contraction of the lithosphere to include depth d variations with latitude ϕ as

$$d(t,\phi) = kt^{1/2} + \sum_{n=0}^{\ell} C_n P_n(\sin\phi) \quad (1)$$

where t is time, P_n are the Legendre polynomials, and C and k are coefficients obtained by least square fitting of the age-depth data for the Pacific.

In consideration of the inferred relation between ridge-axis depth and temperature of the underlying mantle column (*31*) and the well-established relation between ridge-axis topography and degree of melting in the upper mantle (*7*), the long wavelength equatorial topographic minimum of the EPR may also indicate a low degree of melting and a general upper mantle temperature minimum. The same may be the case for the mid-Indian Ridge, which also has an equatorial topographic minimum (*37*). A plot of zero-age bathymetry of the EPR from 20°N to 20°S (Fig. 6B) from recent multi-beam surveys (*38–42*) shows that the crest of the EPR is ~300 m deeper in the equatorial region than to the north and south (*40*). Following the Klein and Langmuir (*7*) relation between ridge depth and mantle temperature, an equatorial EPR 300 m deeper would imply that the subequatorial EPR upper mantle is roughly 100°C colder than that 5° north or south. It follows that available data are consistent with a relatively cold equatorial upper mantle not only in the MAR but also in the EPR and possibly the mid-Indian Ridge. This consistency suggests an equatorial belt of cold upper mantle beneath the oceans.

The equatorial topographic minima of mid-ocean ridges are associated with compensated gravity highs, which are inferred from satellite data (*43*) and indicate an excess mass in the mantle. An equatorial upper mantle that is denser than normal is consistent with lower than normal upper mantle temperatures. Furthermore, the undepleted equatorial upper mantle would contain more Fe, which fractionates relative to Mg into the melt; that is, it would have a higher density than normal sub–mid-ocean ridge depleted mantle (*44, 45*). For instance, extraction of 20 mole percent basaltic melt from pyrolite can decrease the density of the residual mantle by about 2% (*44*).

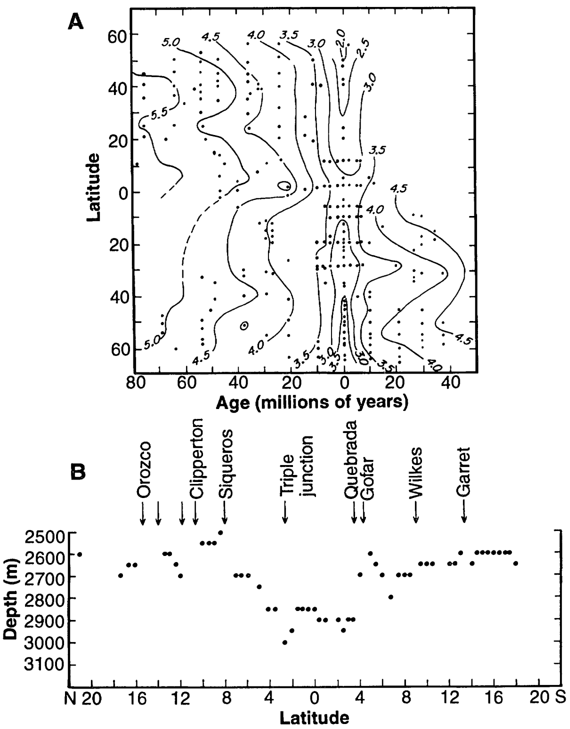

Fig. 6. (**A**) Contour chart of the depth (in kilometers) of the EPR as a function of latitude and age. Dots show the locations of data (*37*). (**B**) Depth below sea level of the crest of the EPR from 20°N to 20°S. Depths are plotted every half degree of latitude and rounded up to the nearest 50 m. Arrows indicate positions of major structural and morphobathymetric discontinuities, such as large transforms and overlappers. Where the Cocos-Nazca boundary meets the EPR is also indicated (triple junction). Most of the data are derived from multibeam surveys (*38–42*).

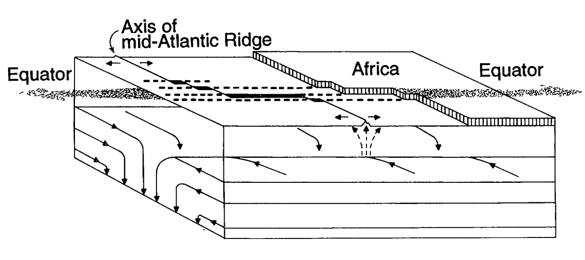

Fig. 7. Model illustrating the suggested downwelling pattern of mantle flow along the equatorial belt of the Atlantic Ocean. Dashed lines indicate the fracture zone trends. Second-order upwelling beneath the axis of the MAR is shown.

The inferred equatorial pattern of cold, dense upper mantle could reflect downwelling mantle flow along the equatorial zone of the oceans (Fig. 7). The equatorial MAR has some similarities to the stretch of mid-ocean ridge between Antarctica and Australia known as the Australian-Antarctic discordance, which is characterized by unusually deep and rough topography, a high density of fracture zones, and an inferred low degree of melting (*46–48*). These features have been attributed to cool mantle and downwelling below the discordance (*46, 48*).

The proposed downwelling beneath the equatorial portion of mid-ocean ridges must be reconciled with shallow upwelling and melting that, although reduced in extent, must occur for a mid-ocean ridge to exist. We adopt a suggestion for the Australian-Antarctic discordance that the shallow upwelling below the ridge is decoupled from the deeper broader pattern of upper mantle convection (*48*). It has been suggested that the Australian-Antarctic discordance marks a boundary between two major chemical-isotopic regions of the upper mantle (*48*). Downwelling at the equator could also constitute a geochemical boundary in the mantle and could explain why the Dupal isotopic anomaly (*49*) is limited essentially to the Southern Hemisphere.

Equatorial Cold Mantle and Earth's Rotation

If downwelling of cold, dense mantle does occur at the equator in the Atlantic, Pacific, and, perhaps, Indian oceans, it can hardly be coincidental and suggests that Earth's rotation influences the geometry of mantle convection. Darwin (*50*) first realized in the last century that the distribution of masses within the Earth affects the location of the spin axis. The effect of density inhomogeneities in the mantle on true polar wander—the shifting of the entire mantle relative to Earth's rotation axis—has been discussed extensively since then (*51–53*).

The subduction of cold, dense lithospheric slabs into Earth's mantle strongly affects true polar wander (*53–55*). Density inhomogenieties in the mantle tend to steer the rotation axis so as to maximize the resulting polar moment of inertia and minimize the kinetic energy of rotation (*52, 53*) A cold (dense) slab sinking in the mantle in a rotating planet induces true polar wander such that the slab tends to be displaced toward the equator if an increase of mantle viscosity with depth is assumed (*53–55*). Such an increase of mantle viscosity with depth is suggested by geoid anomalies over subduction zones (*56*) and other evidence

(*55*). It has been shown that true polar wander has proceeded in some epochs at relatively fast rates, measured in centimeters per year (*57*). If any cold, dense heterogeneity that is present, from whichever source in the convecting upper mantle (for instance, a subducted slab), moves toward the equator at a reasonable rate, the equatorial zone below the ocean basins would tend to be the locus of mantle downwelling and of depressed isotherms. This would prevent significant melting, contributing further to the maintenance of an undepleted, dense equatorial upper mantle in a self-perpetuating pattern.

REFERENCES AND NOTES

1. A. L. Jaques and D. H. Green, *Contrib. Mineral. Petrol.* **73**, 287 (1980).
2. B. O. Mysen and I. Kushiro, *Am. Mineral.* **82**, 52 (1977).
3. A. E. Ringwood, in *Advances in Earth Sciences*, P. Hurley, Ed. (MIT Press, Cambridge, MA, 1966), pp. 287–356.
4. H. J. B. Dick, R. L. Fisher, W. B. Bryan, *Earth Planet. Sci. Lett.* **69**, 88 (1984).
5. P. J. Michael and E. Bonatti, *ibid.* **73**, 91 (1985).
6. E. Bonatti *et al.*, *J. Geophys. Res.* **97**, 4461 (1992).
7. E. M. Klein and C. H. Langmuir, *ibid.* **92**, 8089 (1987).
8. J. G. Schilling, A. N. Davis, D. Fontignie, B. McCully, *Eos* **71**, 624 (1990).
9. E. Bonatti and P. J. Michael, *Earth Planet. Sci. Lett.* **91**, 297 (1989).
10. E. Bonatti, M. Seyler, P. J. Michael, N. Shimizu, in preparation.
11. K. T. M. Johnson, H. J. B. Dick, N. Shimizu, *J. Geophys. Res.* **95**, 2661 (1990).
12. Modal composition was estimated by point counting under the microscope. We counted >2800 points per sample. Results (%): AT196AE: ol, 61.4; opx, 23.5; cpx, 13.8; and sp, 1.2%. AT196M: ol, 62.2; opx, 23.7; cpx, 12.1; and sp, 1.2.
13. E. Bonatti, G. Ottonello, P. R. Hamlyn, *J. Geophys. Res.* **91**, 599 (1986).
14. E. Jagoutz *et al.*, *Proc. Lunar Planet. Sci. Conf.* **10**, 2031 (1979).
15. F. A. Frey and M. Prinz, *Earth Planet. Sci. Lett.* **38**, 129 (1978).
16. D. Elthon, *J. Geophys. Res.* **97**, 9015 (1992).
17. H. J. B. Dick and T. Bullen, *Contrib. Mineral. Petrol.* **86**, 54 (1984).
18. H. J. B. Dick, *Geol. Soc. London Spec. Publ. 42* (1989), p. 71.
19. F. Boudier and A. Nicolas, *Earth Planet. Sci. Lett.* **76**, 84 (1986).
20. H. Downes, *Geology* **18**, 374 (1990).
21. P. R. Hamlyn and E. Bonatti, *Earth Planet. Sci. Lett.* **48**, 65 (1980).
22. Additional evidence supports the idea that the high spinel Cr/Al ratio of these samples does not reflect a high degree of melting on the mantle but is caused by secondary metasomatic reactions. Some of the samples with high (~45 to 50) spinel 100Cr/(Cr + Al) ratios (for example, sample AT180 from the southern wall of the Romanche transform fault valley) contain spinel inclusions in orthopyroxene with low (~18) values for 100Cr/(Cr + Al). These spinel crystals were presumably protected from metasomatic reactions by being enclosed in orthopyroxene.
23. The basaltic glass samples were recovered from the axial valley of the MAR from 15°N to 15°S during expeditions of the research vessels *Akademik Strakhov* and *B. Petrov* of the Geology and Geochemistry Institutes, respectively, of the Russian Academy of Sciences in Moscow. The major element composition of glasses was carried out with a Camebax Microbeam 4 spectrometer electron probe. The analytical techniques are described by N. M. Sushchevskaya, V. K. Ghevorkyan, N. N. Konoukova, and G. M. Kolesov [*Geochem. Int.* **7**, 953 (1985)]. Intercalibration with the Smithsonian microprobe makes the data from the two labs compatible. The data plotted in Fig. 4 include our Na8 and $Fe^{G}8$ (*24, 25*) values versus latitude, together with values calculated from the Smithsonian Institution MORB-glasses database (*26*) and from (*7, 24*).
24. E. M. Klein and C. H. Langmuir, *J. Geophys. Res.* **94**, 4241 (1989).
25. The algorithms used to calculate Na8 and Fe8 (*7*) are $Na8 = Na_2O + 0.373\ (MgO) - 2.98$ and $Fe8 = FeO + 1.664\ (MgO) - 13.313$. We plotted in Fig. 4 $Fe^{G}8$ rather than Fe8. The $Fe^{G}8$ values are calculated from Na8 and Fe8, with the objective of removing the local variability from the data as discussed in (*24*). The $Fe^{G}8$ values were calculated with the following algorithm (*24*)
$$Fe^{G}8 = 2.033(5.233 - bFe) \quad (2)$$
where $bFe = Na8 - 0.19\ Fe8$.
26. W. G. Melson *et al.*, *Smithson. Contrib. Earth Sci.* **19**, 31 (1977); W. G. Melson and T. O'Hearn, in *The Geology of North America*, P. R. Vogt and B. E. Tucholke, Eds. (Geological Society of America, Boulder, CO, 1986), pp. 117–136.
27. W. G. Melson, E. Jarosevich, R. Cifelli, G. Thompson, *Nature* **215**, 381 (1967).
28. E. Bonatti, A. Chermak, J. Honnorez, in *Deep Drilling Results in the Atlantic Ocean: Continental Margins and Paleoenvironment*, M. Talwani, W. Hay, W. B. F. Ryan, Eds. (American Geophysical Union, Washington, DC, 1979), pp. 239–248.
29. J. Honnorez and E. Bonatti, *Nature* **228**, 850 (1970).
30. Y.-S. Zhang and T. Tanimoto, *Nature* **355**, 45 (1992); *Phys. Earth Planet. Inter.* **66**, 160 (1991); *J. Geophys. Res.* **98**, 9793 (1993); Y.-S. Zhang, thesis, California Institute of Technology, Pasadena, CA (1991).
31. D. McKenzie, *J. Petrol.* **25**, 713 (1984).
32. P. J. Fox and D. G. Gallo, *Tectonophysics* **104**, 205 (1984).
33. S. C. Cande, J. L. LaBrecque, W. F. Haxby, *J. Geophys. Res.* **93**, 13479 (1988).
34. R. L. Parker and D. W. Oldenburg, *Nature* **242**, 137 (1973); B. Parson and J. G. Sclater, *J. Geophys. Res.* **82**, 803 (1977).
35. C. H. Langmuir, J. F. Bender, R. Batiza, *Nature* **322**, 422 (1986).
36. Recoveries of mantle peridotites from the EPR have been exceedingly rare. Therefore, the MORP approach is not possible for the EPR. Major element data for MORB glasses are available for portions of the EPR [see, for instance, J. M. Sinton, S. M. Smaglik, S. S. Mahoney, K. C. MacDonald, *J. Geophys. Res.* **96**, 6133 (1991); J. R. Reynolds, C. H. Langmuir, J. F. Bender, K. A. Kastens, W. B. F. Ryan, *Nature* **359**, 493 (1992)], although they are scarce in the equatorial area. Even if EPR MORB data were more complete, they may not allow ready estimates of short-wavelength variations in the extent of melting along the EPR of the type achieved for the MAR. High-resolution petrological studies of limited parts of the EPR (such as by Reynolds *et al.*) have shown that low-Na normal MORB is mixed with, or emplaced close to, high-Na transitional MORB. This may prevent detection of regional variations of Na8 related to variations of extent of melting along the EPR.
37. H. W. Menard and L. M. Dorman, *J. Geophys. Res.* **82**, 5329 (1977).
38. K. D. Klitgord and J. Mammerickx, *ibid.* **87**, 6725 (1982).
39. P. Lonsdale, *Mar. Geophys. Res.* **3**, 295 (1977); *J. Geophys. Res.* **94**, 12197 (1989).
40. The Galapagos propagating rift impacts the EPR north of 2°N and cannot explain a deepening of the EPR from ~5°N to 5°S. The zero-age equatorial minimum level of the EPR reaches about 3 km below sea level and is shallower by several hundred meters than the level of the equatorial MAR. This may reflect a generally hotter upper mantle beneath the fast-spreading EPR than beneath the slow-spreading MAR, as also inferred by S-wave seismic tomography (*30*) and as suggested by theoretical models [see N. H. Sleep, *J. Geophys. Res.* **80**, 4037 (1975); and S. E. Solomon and D. R. Toomey, *Annu. Rev. Earth Planet. Sci.* **20**, 329 (1992)]. A hotter thermal regime below the EPR might explain qualitatively why the signature of the equatorial thermal minimum is stronger in the MAR than in the EPR.
41. K. MacDonald, J. C. Sempere, P. J. Fox, *J. Geophys. Res.* **89**, 6049 (1984).
42. J. Francheteau and R. D. Ballard, *Earth Planet. Sci. Lett.* **64**, 93 (1983).
43. C. A. Wagner, F. J. Lerch, J. E. Brown, J. H. Richardson, *J. Geophys. Res.* **82**, 901 (1977).
44. T. H. Jordan, in *The Mantle Sample: Inclusions in Kimberlities and Other Volcanics*, F. R. Boyd and H. O. A. Meyer, Eds. (American Geophysical Union, Washington, DC, 1979), pp. 1–14.
45. M. J. O'Hara, *Nature* **253**, 708 (1975).
46. J. K. Weissel and D. E. Hayes, *J. Geophys. Res.* **79**, 2579 (1974).
47. E. M. Klein, C. H. Langmuir, H. Staudigel, *ibid.* **96**, 2089 (1991).
48. E. M. Klein, C. H. Langmuir, A. Zindler, H. Staudigel, B. Hamelin, *Nature* **333**, 623 (1988).
49. S. R. Hart, *ibid.* **309**, 753 (1984); *Earth Planet. Sci. Lett.* **90**, 273 (1988).
50. G. Darwin, *Philos. Trans. R. Soc. London Ser. A* **167**, 271 (1877).
51. W. Munk and G. J. F. MacDonald, *J. Geophys. Res.* **65**, 2169 (1960).
52. P. Goldreich and A. Toomre, *ibid.* **74**, 2555 (1969).
53. D. L. Anderson, *Nature* **297**, 391 (1982); *Theory of the Earth* (Blackwell, Boston, MA, 1989).
54. Y. Ricard, G. Spada, R. Sabadini, *Geophys. J. Int.*, in press.
55. G. Spada, Y. Ricard, R. Sabadini, *Nature* **360**, 452 (1992).
56. B. H. Hager, *J. Geophys. Res.* **89**, 6003 (1984).
57. V. Courtillot and J. Besse, *Science* **237**, 1140 (1987).

58. We are grateful to D. Breger, P. Catanzaro, C. DeArturis, and J. Hanley for help in putting together this paper. Discussions with R. Sabadini and G. Spada were most useful in clarifying our ideas on polar wander. Supported by the National Science Foundation. Contribution No. 5100 from Lamont-Doherty Earth Observatory.